CrossMark

METHODS PAPER

# Simplified Murine 3D Neuronal Cultures for Investigating Neuronal Activity and Neurodegeneration

Steven J. Collins[1] · Cathryn L. Haigh [1]

**Abstract** The ability to model brain tissue in three-dimensions offers new potential for elucidating functional cellular interactions and corruption of such functions during pathogenesis. Many protocols now exist for growing neurones in three-dimensions and these vary in complexity and cost. Herein, we describe a straight-forward method for generating three-dimensional, terminally differentiated central nervous system cultures from adult murine neural stem cells. The protocol requires no specialist equipment, is not labour intensive or expensive and produces mature cultures within 10 days that can survive beyond a month. Populations of functional glutamatergic neurones could be identified within cultures. Additionally, the three dimensional neuronal cultures can be used to investigate tissue changes during the development of neurodegenerative disease where demonstration of hallmark features, such as plaque generation, has not previously been possible using two-dimensional cultures of neuronal cells. Using a prion model of acquired neurodegenerative disease, biochemical changes indicative of prion pathology were induced within 2–3 weeks in the three dimensional cultures. Our findings show that tissue differentiated in this simplified three dimensional culture model is physiologically competent to model central nervous system cellular behaviour as well as manifest the functional failures and pathological changes associated with neurodegenerative disease.

✉ Cathryn L. Haigh
chaigh@unimelb.edu.au

1 Department of Medicine (Royal Melbourne Hospital), Melbourne Brain Centre, The University of Melbourne, 30 Royal Parade, Parkville, Melbourne, VIC 3010, Australia

## Introduction

The architecture of the brain is complex, demonstrating intricately organised neuronal pathways and networks. The structure conferred upon cells by their environmental scaffold governs their functioning and limits how cells receive signals from and react in response to signals from their surrounding cells and environment [1]. Such complexity has posed many problems for modelling brain tissue in vitro but overcoming this obstacle is necessary if our understanding of the functional pathways of the brain and its degeneration during disease are to be adequately understood.

Methods and matrices for growing neurones in three-dimensional (3D) cultures have existed for over 20 years [2, 3]. Being able to generate 3D cultures of neurones has recognised advantages in the laboratory, including understanding cellular communication networks, diffusion of molecules through tissue and "clinical trials in a dish" technology [4, 5]. Recently new applications of 3D culture techniques have been extensively developed for growing neurones in 3D with the aim of reproducing tissue architecture such that function and disease can be explored with minimal need for tissue harvests [6, 7].

It is now well established that the adult brain contains neural stem cells (NSCs), which have a limited capacity to replace brain cells throughout life [8–11]. NSCs can self-renew and are multipotent; they can differentiate into cells

of any central nervous system (CNS) lineage. NSCs can be harvested from mouse brain tissue and cultures expanded under standard incubator conditions, making them a plentiful source of cells for 3D differentiation into CNS tissue [12]. Furthermore, the potential to generate 3D cultures from existing transgenic mouse lines permits use of their respective gene manipulations for investigation of gene function or dysfunction.

Many 3D culture systems have been investigated in recent years; some make use of specifically engineered biopolymers [13, 14], some use natural matrix scaffolds [15, 16], some use chip technology [17–19] and some utilise scaffold-free suspension culture [6]. Each has its own benefits and limitations, and researcher's choice can often be guided by factors such as budget and time commitment. While major caveats in all systems include the lack of vascularisation and structural limitations imposed by the skull, the use of neurones grown in 3D is one step closer to reproducing functioning brain tissue. Herein we describe a simple and inexpensive system for generating functional 3D neuronal cultures from murine NSCs with minimal outlay, no specialist equipment and little manipulation by the researcher.

## Methods

### Neural Stem Cell Harvest and Culture

NSCs were harvested from the brains of three mice at 8 weeks of age, as previously described [20]. NSCs were routinely grown as neurospheres in complete proliferation medium (Stem Cell Technologies, VIC, AUS), supplemented with final concentrations of 10 ng/ml FGF, 20 ng/ml EFG and 2 µg/ml heparin, at 37 °C in a humidified, 5 % $CO_2$ tissue culture incubator. Proliferating neurospheres were maintained in Nunc uncoated flasks (Thermo Fisher Scientific, AUS) to avoid adhesion to the plastic surface. Neurospheres were mechanically passaged every 5–8 days as judged by their diameter and were not allowed to become necrotic at the core. Medium was replenished using a half exchange as often as required to prevent acidification.

### 2D Differentiation

Eightwell-chambered coverslips were coated with poly-D lysine (Sigma-Aldrich, NSW, AUS) for a minimum of 1 h at room temperature and washed once with phosphate buffered saline (PBS, Ca and Mg-free pH7.2; Gibco, Thermo Fisher Scientific) immediately prior to plating. Plates were not permitted to dry out during this procedure. NSCs were collected by centrifugation at 100× g for 5 min, brought into single cell suspension by mechanical dissociation and

washed once in PBS, followed by further centrifugation at 150× g for 5 min, before resuspending in an appropriate volume of complete differentiation medium (Stem Cell Technologies). Cells were seeded at a density of $8 \times 10^4$ cells/well and returned to a standard tissue culture incubator for 10 days differentiation, with a half media exchange every three days.

### 3D Differentiation

Neurospheres were grown to ~150–200 µm in diameter but were not allowed to become necrotic (darkened) within their core. Up to 50 neurospheres were washed in PBS and transferred into 2 ml of differentiation medium per well of an uncoated polystyrene 6-well culture plate (Corning Costar, Sigma-Aldrich). Plates were placed on a rotational mixer at 85 rpm in a standard tissue culture incubator and incubated for 48 h with agitation, then removed from the mixer for 24 h static culture, after which time they resumed agitation as before. Media was exchanged, as a half exchange, every three days.

### Immunofluorescent Staining of 2D Cultures

Fixing and staining of two dimensional (2D) monolayers has been described previously [21, 22]. Antibodies and concentrations were the same as described for 3D immunostaining.

### Fixing and Lipid Clearance of 3D Cultures

Fixing and staining of the 3D cultures was carried out in 8-well chambered coverslip slides (Nunc, Thermo Fisher Scientific). Wells were filled with 300 µl of sterile PBS before transferring cells. For each 3D culture, the pipette tip was cut with sterile scissors to create a wide enough aperture that the 3D culture would not be damaged by shearing forces and 100 µl of media containing the 3D cultures was transferred to the 300 µl of PBS already in the well. Cultures were washed twice more by aspirating half of the PBS and replacing the same volume. For each wash, aspirating from near the cultures was avoided to ensure that they were not damaged and the slide was mildly agitated by tapping to mix. Following the final wash, 200 µl of PBS were aspirated from each well and 200 µl of an 8 % (w/v) paraformaldehyde solution added to fix the cells. Fixation was allowed to proceed for 1 h for small diameter cultures (<2 mm) and 2 h for large (>2 mm) cultures. Following fixation cultures were washed five times by aspirating half of the fixative/wash and replacing it with a fresh equal volume (200 µl) as before, being careful not to damage the cultures. Half of the PBS from the well (200 µl) was removed and replaced with 200 µl of 2×sodium dodecyl sulphate (SDS)

permeabilisation buffer (2 % [w/v] SDS, 0.2 M boric acid, pH 8) resulting in a final 1 % [w/v] SDS/0.1 M boric acid buffer. Cultures were permeabilised at room temperature first for 15 min in the 1 % [w/v] SDS buffer then, following exchange of half of the well volume (200 μl) with fresh PBS, in 0.5 % [w/v] SDS for a further 30 min. Cultures were washed five times using half volume exchanges of PBS.

### Immunofluorescent Staining of 3D Cultures

Blocking was carried out in 10 % [v/v] foetal bovine serum (FBS), 1 % [w/v] bovine serum albumin (BSA, Sigma-Aldrich) in PBS for 1 h at room temperature. Blocking buffer was diluted by a half volume exchange with PBS then aspirated completely, taking care not to damage the culture with the pipette tip. Antibodies were applied in 1 % [v/v] FBS, 1 % [w/v] BSA in PBS at the following concentrations: Neuro Filament-L (NF-L, Thermo Fisher Scientific) 1 in 50; glial fibriliary acidic protein (GFAP, Stem Cell Technologies) 1 in 100; N-methyl-D-aspartate (NMDA) receptor subunit-2B (NR2B, Abcam, AUS) 1 in 50; nestin (Sigma-Aldrich) 1 in 50; doublecortin (DCX, Abcam) 1 in 100; and PrP (prion protein, 03R19, kind gift from Victoria Lawson [23]) 1 in 100. Cultures were incubated for 48 h at 4 °C in a humidified chamber. Following primary antibody incubation, the entire antibody solution was aspirated with care and cultures were washed 3× using half volumes PBS exchanges. The final PBS solution was aspirated entirely before addition of secondary antibody. Secondary antibodies, anti-rabbit Alexa Fluor 488 and anti-mouse Alexa Fluor 647 (Thermo Fisher Scientific), were added diluted 1 in 250 in 1 % [v/v] FBS, 1 % [w/v] BSA in PBS and slides were incubated overnight at 4 °C in the dark. Cultures were washed after secondary antibody incubation as for primary antibodies and then were mounted in 3–4 drops of mounting media with DAPI (Sigma-Aldrich). A pipette tip was used to position the culture within the well then mounting medium was cured overnight at room temperature before imaging.

### Confocal Imaging

Confocal imaging was carried out using a Leica SP8 confocal microscope as described in [24]. Z-projections were generated using Fiji (ImageJ 1.50d) imaging software [25]. Images shown are representative of cultures generated from >3 independent differentiations unless otherwise stated.

### Caspase Imaging

The manufacture and characterisation of the Near Infra-Red (NIR)-VAD-fmk probe have been described previously [26]. Live cultures were incubated with 2.5 μM NIR-VAD-fmk for 30 min then imaged using a Nikon Eclipse TE2000-E epi-fluorescence microscope (Nikon-Roper Scientific, Coherent Scientific, AUS). Following imaging cultures were transferred to fresh media for continued incubation. Image analysis was done using NIS-Elements imaging software (Nikon-Roper Scientific).

### Calcium Influx Assay

Cultures were collected by centrifugation at 100× g for 5 min. Using a cut pipette tip, 3–4 organoids per well were transferred into a 96-well plate in 100 μl of fresh differentiation medium. Using the Fluo-4 Direct™ Calcium Assay Kit (Thermo Fisher Scientific), at the beginning of the assay 100 μl of calcium assay working buffer was prepared as per manufacturer's instructions and was added to each test well. Plates were incubated for 1 h with readings taken using 488 nm excitation and 530 nm emission filters in a FluoSTAR Optima (BMG Labtech, AUS), the basal rate of calcium influx was calculated once a linear relationship was stable. After basal calcium flux had been determined, 10 mM glutamate (Sigma-Aldrich) was added and readings were taken for further 2 h. Rates were calculated as linear tangents to the curve using MARS analysis software (BMG Labtech).

### Prion Infections

Brain homogenates from M1000 prion strain [27] infected and sham inoculated, "mock" infected mice were prepared as a 10 % (w/v) stock in PBS. Prion and mock infection were induced within the 3D cultures by including infected and mock homogenates in normal culture media at a final concentration of 0.01 % (w/v) for 72 h.

### Thioflavin-T (ThT) Staining

Cultures were incubated in normal media containing 10 μM ThT (Sigma-Aldrich) with agitation for 30 min before fixing as described above.

## Results and Discussion

### Morphology of Cultures Differentiated in 3D

Three-dimensional cultures of CNS tissue were generated using neurospheres of murine NSCs that had been grown to the size limit of the culture (~150–200 μm) without being allowed to become necrotic at their core. Using the principle of culture agitation previously described for generating 3D cultures of neuronal cells [15] at induction of

**Fig. 1** Differentiation and morphology of neuronal 3D cultures. **a** Schematic of the 3D differentiation protocol and expression of cellular markers during maturation. **b** Examples of culture size and morphology, presented in wells of a 24-well plate. Well diameter is indicated and *red arrows* and *brackets* indicate the position of cultures of varying size. Immunofluorescent staining of whole cultures differentiated without **c** or with 1 μg/ml laminin **d** in the differentiation medium. A selection of individual stack channels are shown with z-projection merges. Neurones are labelled by NF-L (*red*) staining, astrocytes by GFAP (*green*) and cell nuclei by DAPI (*blue*) uptake. Scale bars = 50 μm
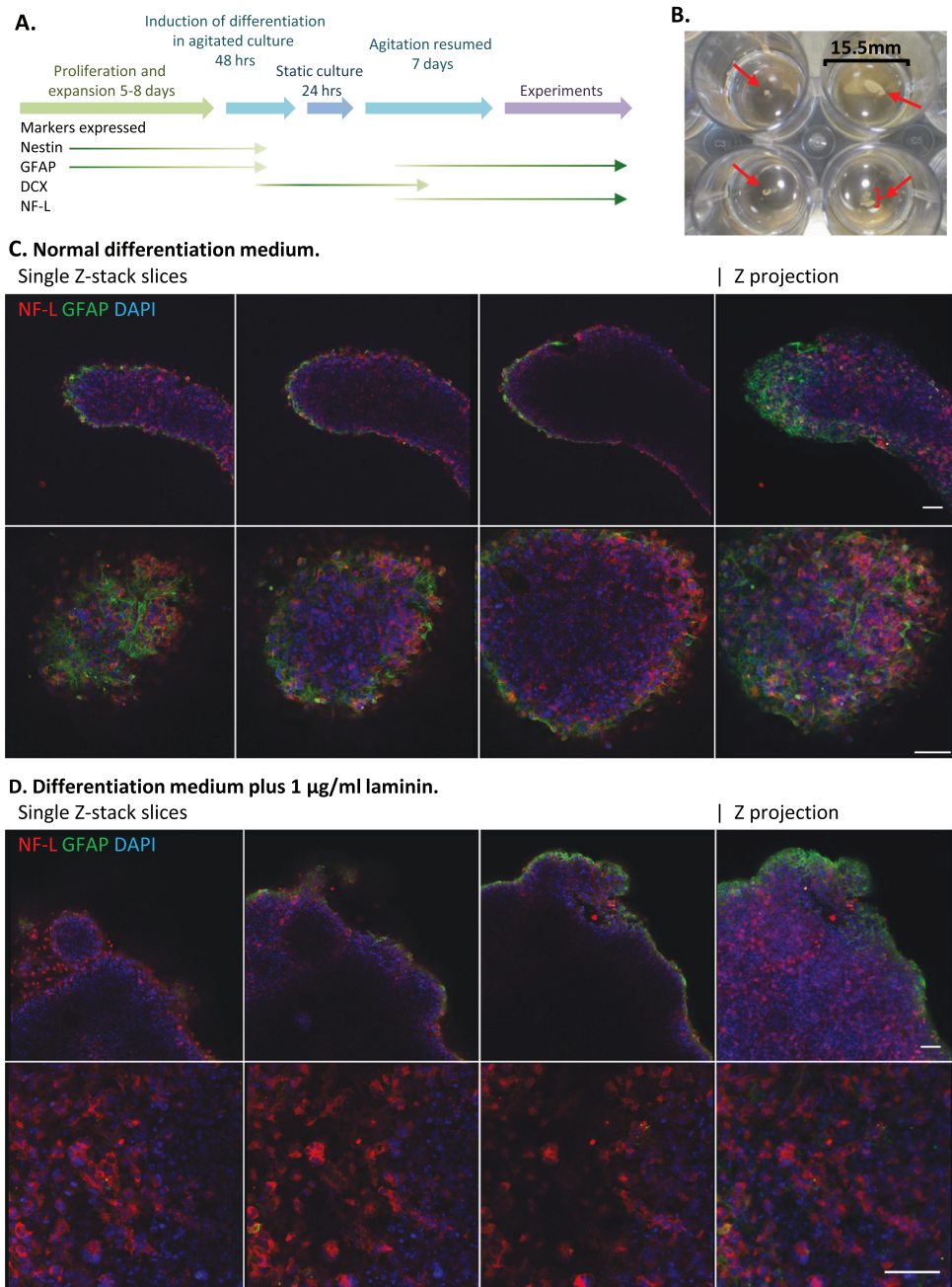


differentiation, neurospheres were constantly stirred by orbital mixing followed by a static period and then further agitated incubation. The experimental protocol is shown in Fig. 1a. Two dimensional cultures reach maturity (as detected by markers of mature neurones) by 7 days' differentiation. Since the cores of the 3D cultures were not accessible to the differentiation medium, so diffusion of signals would need to occur from the sphere surface, differentiation was allowed to proceed for several days longer (to 10 days) before assessment of the cellular populations. Visual inspection of the cultures indicated that once

maturity was reached, they did not continue to expand in size and neither did they shrink with age in the time period considered. Fig. 1b shows brightfield morphology of 3D cultures. Immunostaining for neurones and astrocytes demonstrated an outer astrocytic layer, wrapping around the culture with a denser neuronal stratum underneath (Fig. 1c). The neuronal:astrocytic ratio of the cells could be influenced towards neurones by including 1 μg/ml laminin in the culture medium during differentiation (Fig. 1d).

Crude structural formations were observed with protuberances reminiscent of lobes budding from the periphery

**Fig. 2** Comparison of cellular maturity between 2D and 3D cultures. Cultures were differentiated in 2D and 3D for 10 days as per the respective differentiation protocols and immature cells detected with antibodies against **a** nestin (*green*) and **b** DCX (*green*) as compared with mature neurones (NF-L; *red*). Cell nuclei are labelled with DAPI (*blue*). Scale bar = 100 µm
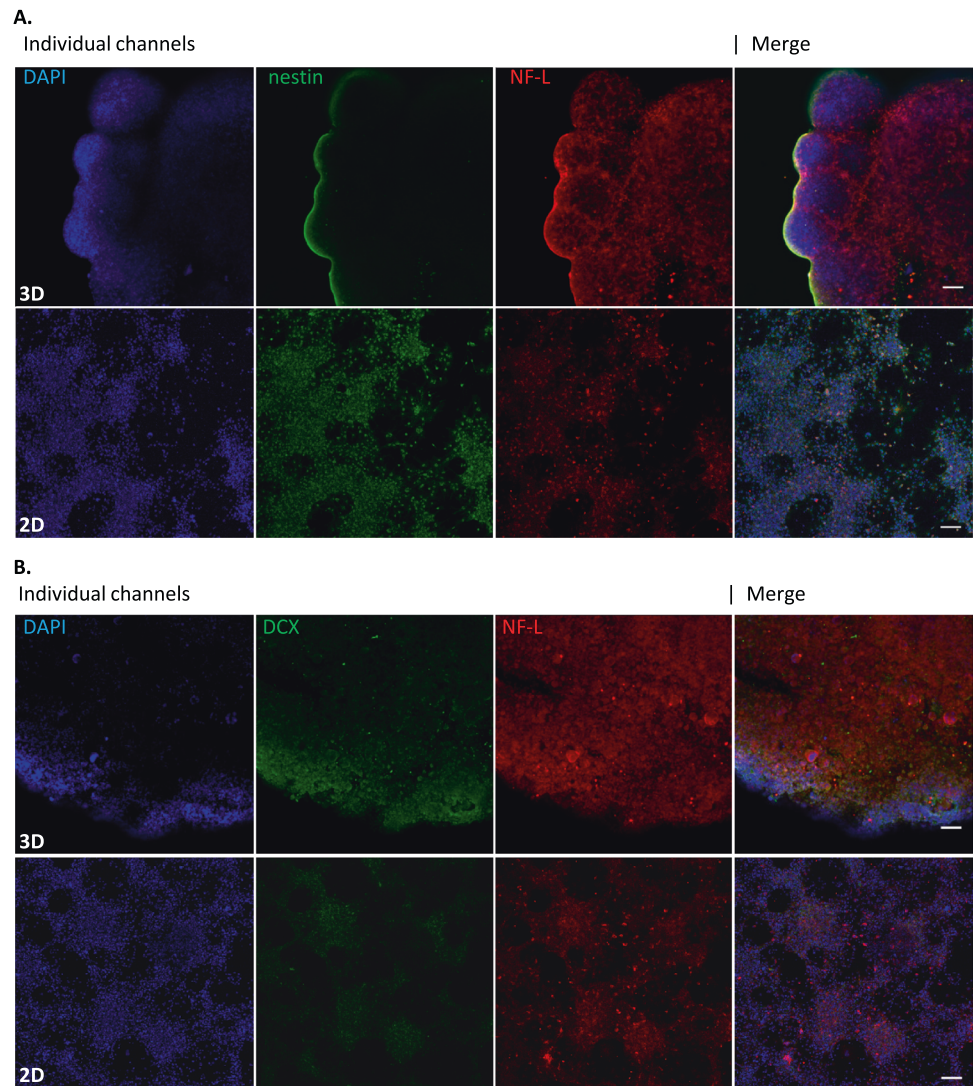


of the cultures and regions of overlaid dense cells. Some of the structural formations appeared to be due to the agitation causing distension of culture boundaries and some looked as if due to several cultures fusing together and wrapping around each other with neurones appearing to line up along the interfaces. It was apparent that agitation was required for the structural adhesion of cultures as those differentiated in non-agitated suspension cultures were fragile, breaking apart on manipulation (data not shown).

**Comparison of Cell Populations Within 2D and 3D Cultures Shows Increased Neuronal Differentiation in 3D**

To determine how successful the differentiation of the 3D cultures had been as compared with neuronal populations achievable in 2D differentiations, parallel cultures were differentiated in 2D and 3D (without additional laminin) for

10 days and compared for markers of NSCs (nestin; Fig. 2a), neural precursors (DCX; Fig. 2b) and mature neurones (NF-L); expression profiles relative to neuronal maturity are shown in Fig 1a. Qualitative assessment of the staining intensity indicated that greater neuronal signal is observed in the 3D cultures. This observation is consistent with human 3D culture systems that also report increased neuronal content over 2D differentiation [28]. In 3D cultures, immature cells are localised nearer the surface of the culture rather than throughout as seen in the 2D cultures. Visual inspection shows that the most of the immature NSCs (nestin positive) are most externally located, with the neuroblasts (DCX positive) located as a layer between nestin and the NF-L stained mature neurones. As compared with the 2D differentiations, the 3D cultures display less nestin staining but comparatively more DCX indicating that less of the cells cultured in 3D have failed to differentiate and more have committed to neuronal lineage. The external

localisation of the nestin-positive NSCs is alongside the region where GFAP was detected and, while the staining pattern differs between the GFAP and nestin antibodies, there may be some GFAP staining of the cultures that is due to expression of GFAP in immature NSCs. Since no further expansion of the cultures was observed following differentiation, the immature cells on the periphery of the culture might be senescent, quiescent awaiting specific growth/ differentiation signals, incapable of differentiation or performing as yet an unknown function for the maintenance of the culture.

### Production of Neuronal Subsets within the 3D Cultures

For the 3D cultures to be useful models, they must demonstrate cell functionality. To consider whether functional neuronal subsets were being produced within the culture, the activity of glutamatergic neurones was measured by calcium flux prior to and following stimulation with glutamate. Significant calcium influx was observed upon glutamate challenge (Fig. 3a), indicating that functional glutamatergic neurones reside within the cultures. For visualisation of glutamatergic neurones, cultures were stained for expression of the NR2B. The staining showed strong signal mostly towards the periphery of the culture with some dense areas inside the core (Fig. 3b). Contour intensity plots were generated for comparison of the positioning of the glutamatergic neurones with the other cellular subsets within the culture. Regions of interest were gated at the periphery of the culture (Fig. 4a) and within the core (Fig. 4b). These plots show a clear, narrow nestin positive region at the outer edge of the culture. Inside of this was a layer of astrocytes/GFAP-positive cells and neuronal precursors intermingled with mature neurones, including the glutamatergic neurones. The neurones extended further

into the tissue and only neurones were detected within the core, with small puncta of glutamatergic staining. The layer summary schematic is shown in Fig 4c.

### Cultures Survive for up to 6 Weeks

To determine culture longevity and the reasonable window for experimentation, cellular attrition in the 3D cultures was monitored over time. The cultures were incubated with a near-infra-red (NIR), pan-caspase imaging probe at 1, 3 and 6 weeks following culture induction (Fig. 5a-c). A NIR probe was employed in these assays because when neuronal tissue degenerates lypofuscin is produced, which fluoresces through the green-red wavelength range and can mask the genuine signal from many imaging probes [26]. Caspase probe intensity was monitored relative to autofluorescence background (Fig. 5d) and very low uptake of the pan-caspase probe was observed at 3 weeks (Fig. 5b) with the staining pattern diffuse, indicative of background binding. Attrition of the culture, seen as punctate staining of individual cells within localised regions, became apparent at 6 weeks (Fig. 5c).

### Induction of a Neurodegenerative Disease Phenotype

A particular advantage to 3D neuronal cultures is the possibility of modelling neurodegenerative diseases, which often have hallmark features that cannot be detected in 2D monolayer cultures even of primary neurons. To determine whether the 3D neuronal cultures could develop disease pathology, we induced a neurodegenerative disease phenotype.

Prion diseases are transmissible neurodegenerative diseases. The transmissibility of prion diseases offers an advantage for the study of neurodegeneration as infection (and therefore neurodegeneration) can be transmitted from culture to culture. However, very few secondary cell lines show overt abnormalities or monitorable prion pathology, instead displaying only propagation of the protein agent. NSCs cultures have previously been shown to have utility as models of prion infection. NSCs can propagate prions both when growing and following differentiation into mature CNS cells [29, 30]. Furthermore, using our NSC model, toxic changes are seen in differentiated neurones and astrocytes when exposed to prions [20, 22]. Prion infection was induced within the 3D cultures by a single 72 h exposure to the M1000 prion strain [27] from infected mouse brain homogenates (0.01 % [w/v] final concentration), with normal, uninfected brain homogenates used to treat "mock" control cultures. Three weeks post-infection, cultures were fixed and stained to look for changes in their neuronal/astrocytic morphology. No overt change could be seen in the neuronal population, however
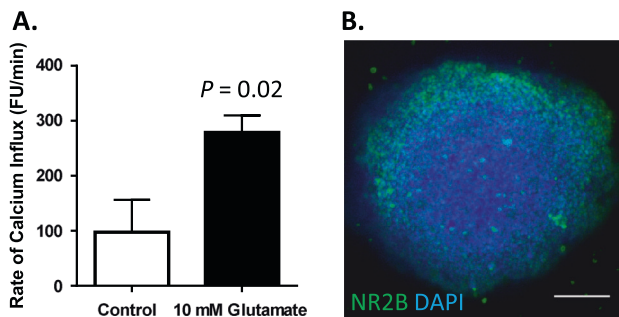
**Fig. 3** Culture function. **a** Calcium influx assay comparing culture response before and after stimulation with glutamate. Graph shows mean and s.e.m. of the rates. Students *t*-test, $t = 3.134$, n = 4. **b** Immunofluorescent staining of glutamatergic neurones in the culture detected using the NR2B (*green*). Nuclei are stained with DAPI in *blue*. Scale bar = 100 μm
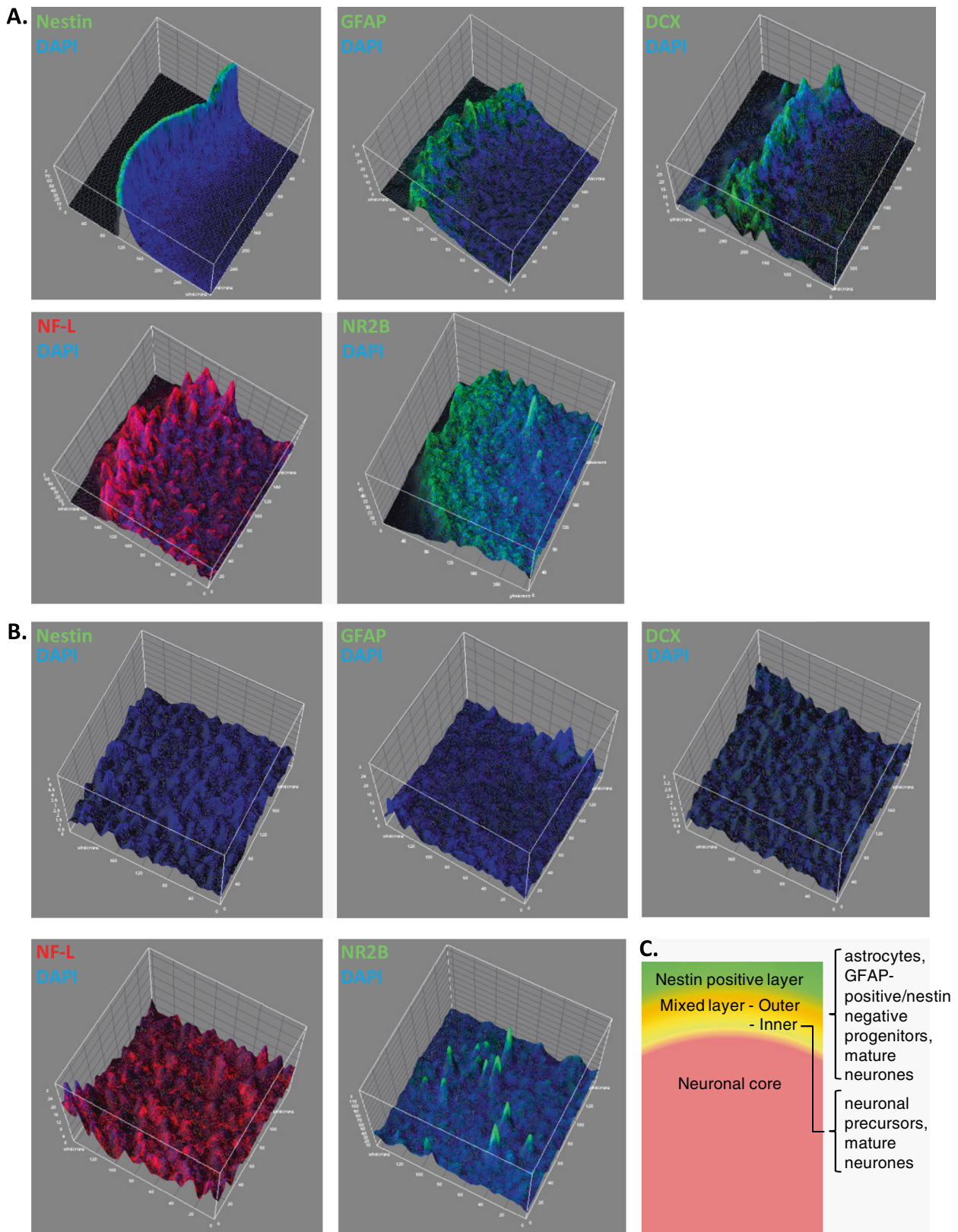
**Fig. 4** Culture layers. Intensity contour plots of **a** culture periphery and **b** culture core for comparison of marker distribution. Nestin, GFAP, DCX and NR2B are shown in *green*, DAPI in *blue* and NF-L in *red*. **c** Schematic of culture layer composition

astrocytes surrounding the infected culture exterior appeared to show reduced GFAP staining and displayed altered morphology (Fig. 6).
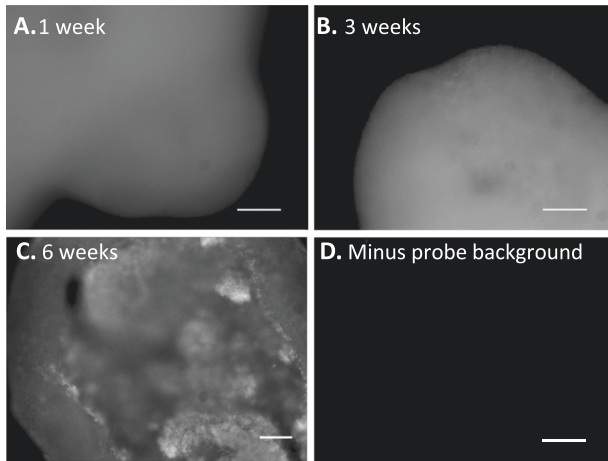


**Fig. 5** Culture viability. Cultures were incubated with NIR-VAD-fmk pan-caspase probe at 1 **a** 3 **b** and 6 **c** weeks post-differentiation. **d** Background fluorescence of the culture in the absence of probe collected under identical imaging conditions. Scale bar = 100 μm

Reduced detection of astrocytes appears contrary to the astrocytosis reported in prion disease, however, there may be a number of factors contributing to the reduced staining such as: expression of PrP in astrocytes changes their isoform expression profiles [21] and this may also occur upon infection, changing GFAP detection; 3 weeks may be a too short time period to detect astrocyte proliferation; astrocytes play a role in re-modelling the extra-cellular matrix during the times of disease or stress [31] and this could result in changed astrocytic adhesion, which, in the absence of the structure imposed by the dense CNS neuropil and extra-cellular matrix interstitium, might cause these cells to be lost into the surrounding media; the astrogliosis associated with prion disease also involves the recruitment of microglia [32], which stimulates astrocyte proliferation [33] and in the absence of their signals, the astrocytes may not be stimulated to grow—further co-culture experiments will be required to assess this role (note that microglia do not differentiate from NSCs but are derived from the bone marrow and so should not be present in our cultures). Further, during human prion disease, hypertrophic astrocytes show two morphologies, glial fibril containing and a subset

**Fig. 6** Morphology of 3D cultures following exposure to prions. Cultures were incubated for 22 days following exposure to infectious prion or mock control brain homogenate and stained for neuronal and astrocytic content. For each, two magnifications are shown (*upper* panels scale bar = 100 μm / *lower* panels scale bar = 20 μm) with channels split into nuclei (DAPI; *blue*), astrocytes (GFAP; *green*) and neurones (NF-L; *red*) alongside the merged image as indicated
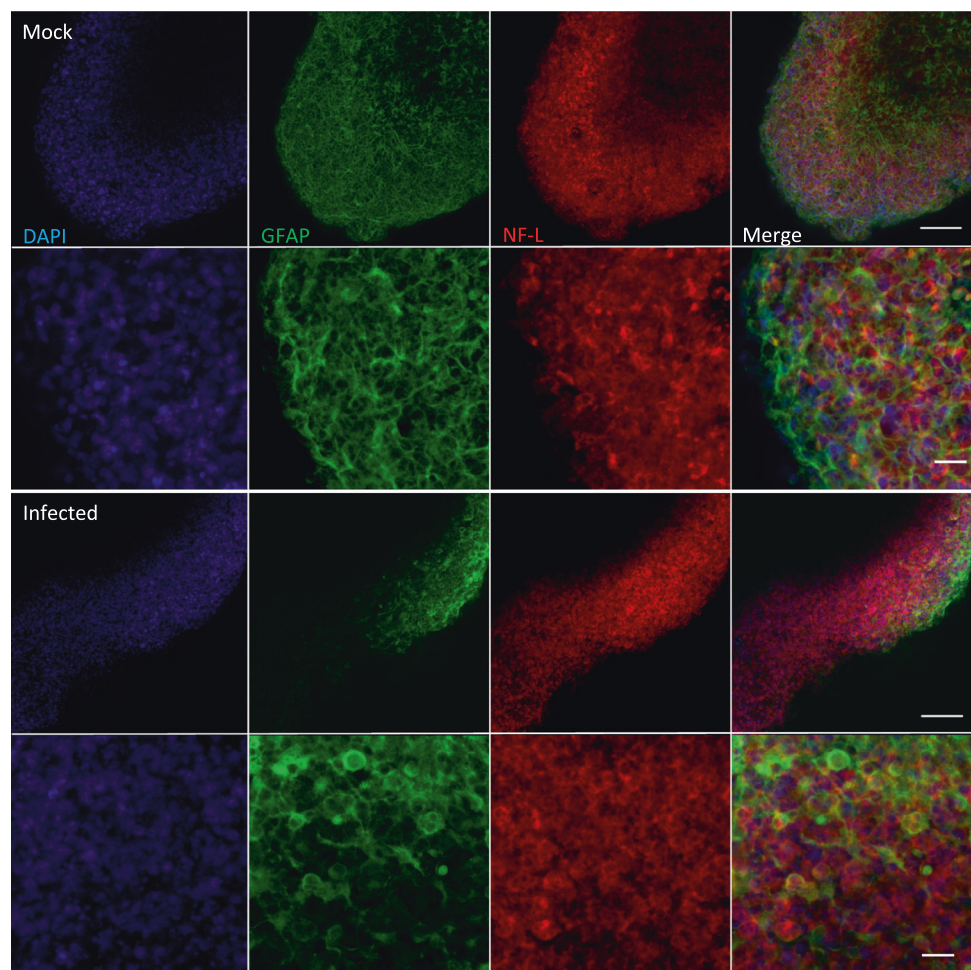
**Fig. 7** 3D cultures develop a prion neurodegenerative phenotype. **a** Culture death, as shown by incubation with the pan-caspase probe NIR-VAD-fmk, indicates accelerated attrition in the cultures exposed to prion infection. **b** Heat plot of regions of heightened caspase activation extending into the tissue from the culture surface. Intensity scale is shown *right*. **c** Incubation of cultures with ThT (*cyan*) at 22 dpi and immunofluorescent staining for neurones (NF-L; *red*; *left* panels scale bar = 100 μm, *right upper* and *lower* scale bar = 50 μm, *right middle* panel scale bar = 20 μm). Cell nuclei are stained with DAPI (*blue*). **d** Immunofluorescent staining of cultures at 22 dpi for PrP (*green*) and NF-L (*red*; nuclei shown with DAPI in *blue*) shows increased PrP staining and punctate deposits in the infected cultures. Scale bars = 50 μm. Representative images are shown from 4 independent differentiations in A and 2 each of these were used for staining in C and D
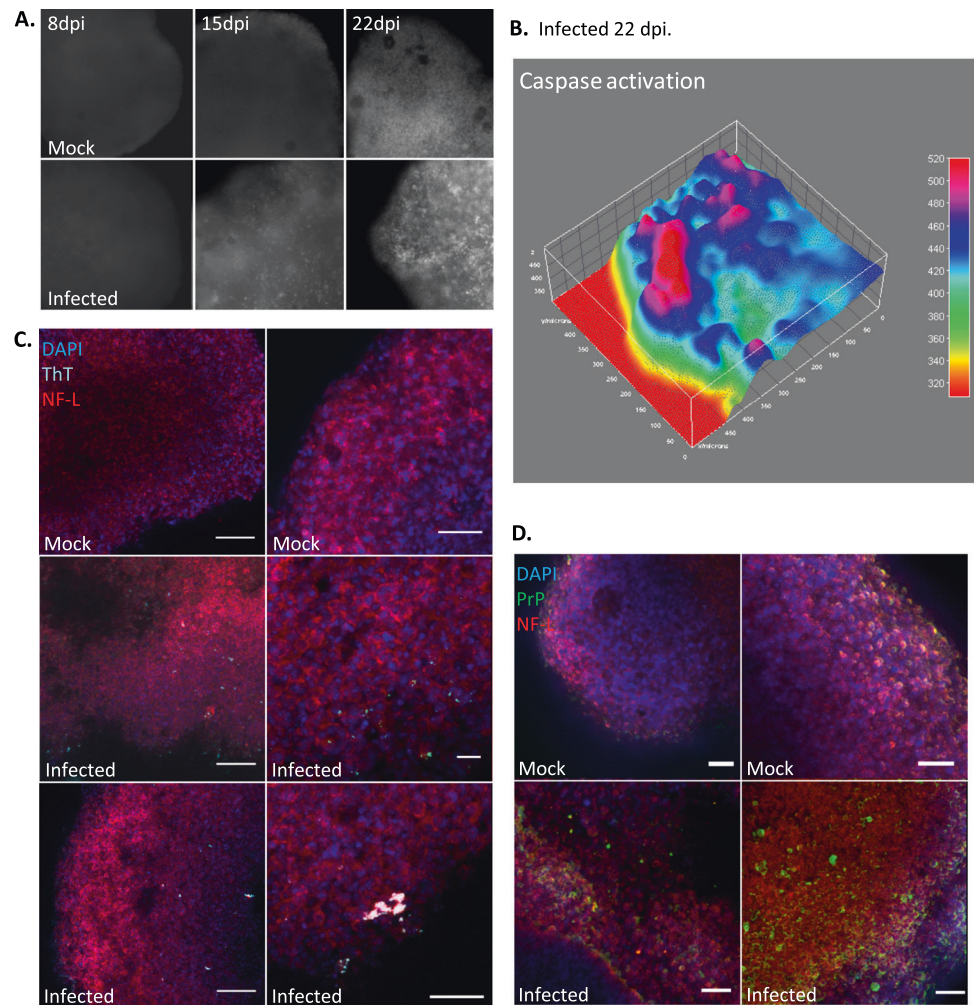


showing suboptimal fixation resulting in a "watery" cytoplasm appearance [34]—the astrocytes in the 3D cultures may be the latter subset resulting in apparently reduced GFAP detection. Finally, astrocytes die following astrogliosis in certain forms of brain injury [35–37] and, in the case of our 3D cultures, the infection (accumulation of prions [38] and markers of cell damage [39] are known to occur in astrocytes) may have tipped astrocytes from a helpful response to cell death. These unknowns further demonstrate the potential information that can be ascertained by assaying CNS cells in 3D rather than monolayer culture.

Cell death in the brains of prion infected mice, as shown by caspase activation, can be detected in neurones residing within the hippocampus and thalamus, and is found in close proximity to PrP deposition [40]. To assess if prion infection results in accelerated culture death, cultures were imaged following incubation with the NIR pan-caspase probe at 8, 15 and 22 days post infection (dpi) to determine if the culture was displaying prion-induced cell death. Significantly, more caspase puncta were observed in the

cultures exposed to prions than those receiving the mock treatment and this was obvious by 15 dpi and dramatically increased by 22 dpi (Fig. 7a). A heat map of capase activation at 22 dpi shows that very little caspase activation occurs within the outer layer of the culture but regions of heightened activation arise through the mixed layer and extends into the neuronal core (Fig. 7b). The 22 dpi cultures were fixed for immunostaining either with (Fig. 7c) or without incubation with ThT to identify deposits of aggregated protein. Cultures without ThT staining were incubated with antibodies against the PrP to directly identify PrP deposits (Fig. 7d). Examination of the cultures showed deposits of PrP replicating plaque formation. PrP detection was increased in the infected cultures, which is observed as mis-folded PrP accumulates both in human disease and animal models of disease [41, 42]. Comparison with 3D cultures generated from prion knock-out NSCs showed that the PrP detected is not due to persistence of the original inoculums (Sup Fig. 1). The ThT-positive aggregates and PrP-staining deposits were lying within neuron-dense regions of the culture and also alongside the boarders of

these regions, which may represent formation at the periphery of the neuronal population or within regions too dense for the antibody staining to penetrate (Fig. 7c/d). A further observation was that DAPI staining became less distinct in the infected cultures suggesting that the nuclear material may be breaking down as part of the toxicity of infection.

The formation of ThT-reactive protein deposits shows that the mechanisms impaired in the brain during neurodegenerative diseases are equally affected when neurones are cultured in 3D and therefore the 3D cultures can be used to examine these failures in vitro. This could have potential applications for investigating other neurodegenerative diseases where plaque formation is a hallmark, such as Alzheimer's Disease (AD). As NSCs can be harvested from the brain of any mouse, transgenic AD mouse models could be utilised to make these cultures for such research. Validations of potential therapeutics targeting mitigation of protein deposition can be examined in this system for their capacity to prevent or clear protein deposits before human in vivo trial. Furthermore, the ease of their production and relatively minimal time scales to produce cultures permit many validations to be performed quickly and cheaply.

## Conclusions

Growing neurones from NSCs in 3D offers a number of advantages over traditional primary cultures. Herein, we developed a neuronal 3D culture system that was relatively inexpensive and time efficient. NSCs can be harvested from the brains of adult mice or from developing embryos. Therefore, NSC lines can be made containing any mutation that can be engineered into a mouse. Ethical, logistical and cost advantages for using these cells include that they can be expanded to produce differentiated cultures on demand and cryopreserved for longevity, thereby reducing the numbers of mice needed for harvests, the time taken for repeated harvests and the costs of maintaining mouse colonies. Our simple and relatively inexpensive approach for growing murine CNS tissue in 3D produces cultures with good longevity that can be used to study neuronal function. It further offers a system for investigating the pathogenesis and biochemical pathways of disease that cannot be studied in 2D and a potential model for therapeutic compound screening, wherein changes in 3D readouts may more reliably reproduce changes observed in vivo.

## References

1. Bard, J., & Elsdale, T. (1986). Growth regulation in multilayered cultures of human diploid fibroblasts: The roles of contact, movement and matrix production. *Cell and Tissue Kinetics*, *19*(2), 141–154.
2. Bellamkonda, R., et al. (1995). Hydrogel-based three-dimensional matrix for neural cells. *Journal of Biomedical Materials Research*, *29*(5), 663–671.
3. Justice, B. A., Badr, N. A., & Felder, R. A. (2009). 3D cell culture opens new dimensions in cell-based assays. *Drug Discovery Today*, *14*(1–2), 102–107.
4. Haston, K. M., & Finkbeiner S. (2016). Clinical trials in a dish: The potential of pluripotent stem cells to develop therapies for neurodegenerative diseases. *Annual Review of Pharmacology and Toxicology*, *56*, 489–510.
5. Lai, Y., Cheng, K., & Kisaalita, W. (2012). Three dimensional neuronal cell cultures more accurately model voltage gated calcium channel functionality in freshly dissected nerve tissue. *PLoS One*, *7*(9), e45074.
6. Pasca, A. M., et al. (2015). Functional cortical neurons and astrocytes from human pluripotent stem cells in 3D culture. *Nature Methods*, *12*(7), 671–678.
7. Terrasso, A. P., et al. (2015). Novel scalable 3D cell based model for in vitro neurotoxicity testing: Combining human differentiated neurospheres with gene expression and functional endpoints. *Journal of Biotechnology*, *205*, 82–92.
8. Emsley, J. G., et al. (2005). Adult neurogenesis and repair of the adult CNS with neural progenitors, precursors, and stem cells. *Progress in Neurobiology*, *75*(5), 321–341.
9. Kitabatake, Y., et al. (2007). Adult neurogenesis and hippocampal memory function: new cells, more plasticity, new memories? *Neurosurgery Clinics of North America*, *18*(1), 105–113. x.
10. Lugert, S., et al. (2010). Quiescent and active hippocampal neural stem cells with distinct morphologies respond selectively to physiological and pathological stimuli and aging. *Cell Stem Cell*, *6*(5), 445–456.
11. Wang, Y. Z., et al. (2011). Concise review: Quiescent and active states of endogenous adult neural stem cells: Identification and characterization. *Stem Cells*, *29*(6), 907–912.
12. Ahlenius, H., & Kokaia, Z. (2010). Isolation and generation of neurosphere cultures from embryonic and adult mouse brain. *Methods in Molecular Biology*, *633*, 241–252.
13. Bosi, S., et al. (2015). From 2D to 3D: novel nanostructured scaffolds to investigate signalling in reconstructed neuronal networks. *Scientific Reports*, *5*, 9562.
14. Lu, H. F., et al. (2012). Efficient neuronal differentiation and maturation of human pluripotent stem cells encapsulated in 3D microfibrous scaffolds. *Biomaterials*, *33*(36), 9179–9187.
15. Lancaster, M. A., & Knoblich, J. A. (2014). Generation of cerebral organoids from human pluripotent stem cells. *Nature Protocols*, *9*(10), 2329–2340.
16. Labour, M. N., et al. (2016). 3D compartmented model to study the neurite-related toxicity of Abeta aggregates included in collagen gels of adaptable porosity. *Acta Biomater*, *37*, 38–49.

17. Anene-Nzelu, C. G., et al. (2013). Scalable alignment of three-dimensional cellular constructs in a microfluidic chip. *Lab on a Chip, 13*(20), 4124–4133.

18. Moreno, E. L., et al. (2015). Differentiation of neuroepithelial stem cells into functional dopaminergic neurons in 3D microfluidic cell culture. *Lab on a Chip, 15*(11), 2419–2428.

19. Seidel, D., et al. (2012). Induced tauopathy in a novel 3D-culture model mediates neurodegenerative processes: A real-time study on biochips. *PLoS One, 7*(11), e49150.

20. Haigh, C. L., et al. (2011). Acute exposure to prion infection induces transient oxidative stress progressing to be cumulatively deleterious with chronic propagation in vitro. *Free Radical Biology & Medicine, 51*(3), 594–608.

21. Collins, S. J., et al. (2015). The prion protein regulates beta-amyloid mediated self-renewal of neural stem cells in vitro. *Stem Cell Research & Therapy, 6*(1), 60.

22. Sinclair, L., et al. (2013). Cytosolic caspases mediate mislocalised SOD2 depletion in an in vitro model of chronic prion infection. *Disease Models & Mechanisms, 6*(4), 952–963.

23. Lawson, V. A., et al. (2008). Mouse-adapted sporadic human Creutzfeldt-Jakob disease prions propagate in cell culture. *The International Journal of Biochemistry & Cell Biology, 40*(12), 2793–2801.

24. Haigh, C. L., McGlade, A. R., & Collins, S. J. (2015). MEK1 transduces the prion protein N2 fragment antioxidant effects. *Cellular and Molecular Life Sciences : CMLS, 72*(8), 1613–1629.

25. Schindelin, J., et al. (2012). Fiji: An open-source platform for biological-image analysis. *Nature Methods, 9*(7), 676–682.

26. Lawson, V. A., et al. (2010). Near-infrared fluorescence imaging of apoptotic neuronal cell death in a live animal model of prion disease. *ACS Chemical Neuroscience, 1*(11), 720–727.

27. Brazier, M. W., et al. (2006). Correlative studies support lipid peroxidation is linked to PrP(res) propagation as an early primary pathogenic event in prion disease. *Brain Research Bulletin, 68*(5), 346–354.

28. Choi, S. H., et al. (2014). A three-dimensional human neural cell culture model of Alzheimer's disease. *Nature, 515*(7526), 274–278.

29. Herva, M. E., et al. (2010). Prion infection of differentiated neurospheres. *Journal of Neuroscience Methods, 188*(2), 270–275.

30. Milhavet, O., et al. (2006). Neural stem cell model for prion propagation. *Stem Cells, 24*(10), 2284–2291.

31. Jones, E. V., & Bouvier, D. S. (2014). Astrocyte-secreted matricellular proteins in CNS remodelling during development and disease. *Neural Plasticity, 2014*, 321209.

32. Marella, M., & Chabry, J. (2004). Neurons and astrocytes respond to prion infection by inducing microglia recruitment. *The Journal of Neuroscience, 24*(3), 620–627.

33. Brown, D. R. (2001). Microglia and prion disease. *Microscopy Research and Technique, 54*(2), 71–80.

34. Liberski, P. P., & Brown, P. (2004). Astrocytes in transmissible spongiform encephalopathies (prion diseases). *Folia neuropathologica / Association of Polish Neuropathologists and Medical Research Centre, Polish Academy of Sciences, 42*(Suppl B), 71–88.

35. Takuma, K., Baba, A., & Matsuda, T. (2004). Astrocyte apoptosis: implications for neuroprotection. *Progress in Neurobiology, 72*(2), 111–127.

36. Szydlowska, K., Zawadzka, M., & Kaminska, B. (2006). Neuroprotectant FK506 inhibits glutamate-induced apoptosis of astrocytes in vitro and in vivo. *Journal of Neurochemistry, 99*(3), 965–975.

37. Saas, P., et al. (1999). CD95 (Fas/Apo-1) as a receptor governing astrocyte apoptotic or inflammatory responses: A key role in brain inflammation? *Journal of Immunology, 162*(4), 2326–2333.

38. Diedrich, J. F., et al. (1991). Scrapie-associated prion protein accumulates in astrocytes during scrapie infection. *Proceedings of the National Academy of Sciences of the United States of America, 88*(2), 375–379.

39. Andreoletti, O., et al. (2002). Astrocytes accumulate 4-hydroxynonenal adducts in murine scrapie and human Creutzfeldt-Jakob disease. *Neurobiology of Disease, 11*(3), 386–393.

40. Drew, S. C., et al. (2011). Optical imaging detects apoptosis in the brain and peripheral organs of prion-infected mice. *Journal of Neuropathology and Experimental Neurology, 70*(2), 143–150.

41. Meyer, R. K., et al. (1986). Separation and properties of cellular and scrapie prion proteins. *Proceedings of the National Academy of Sciences of the United States of America, 83*(8), 2310–2314.

42. Muramoto, T., et al. (1992). The sequential development of abnormal prion protein accumulation in mice with Creutzfeldt-Jakob disease. *The American Journal of Pathology, 140*(6), 1411–1420.